



*Research article*

## Effect of adaptive rewiring delay in an SIS network epidemic model

Jing Li<sup>1,2,3</sup>, Zhen Jin<sup>2,3,\*</sup> and Yuan Yuan<sup>2,4,\*</sup>

<sup>1</sup> School of Applied Mathematics, Shanxi University of Finance and Economics, Taiyuan Shanxi 030006, China

<sup>2</sup> Complex Systems Research Center, Shanxi University, Taiyuan Shanxi 030006, China

<sup>3</sup> Shanxi Key Laboratory of Mathematical Techniques and Big Data Analysis on Disease Control and Prevention, Shanxi University, Taiyuan, Shanxi 030006, China

<sup>4</sup> Department of Mathematics and Statistics, Memorial University of Newfoundland, St. John's, Newfoundland, A1C 5S7, Canada

\* **Correspondence:** Email: jinzhn@263.net, yyuan@mun.ca.

**Abstract:** In the real world, in order to avoid the infection risk, people tend to cut off the links with their infected neighbors, then look for other susceptible individuals to rewire. However, the rewiring process does not occur immediately, but takes some time. We therefore establish a delayed SIS network model with adaptive rewiring mechanism and analyze the long-term steady states for the system with and without the rewiring delay. We find that with the rewiring time, there are infinite equilibria lie on a line in a high-dimensional state space, which is quite different from normal delayed model. The numerical simulation results show that the system approaches to different steady state on the line under the same initial values and different rewiring delays, and the stable limit cycle can appear with the increase of rewiring delay. These surprising results may provide new insights into the study of delayed network epidemic model.

**Keywords:** SIS network epidemic model; adaptive rewiring; time delay; line equilibria

---

### 1. Introduction

The so-called network is composed of many nodes and edges connecting the two nodes, where nodes and edges are used to represent objectives and relationships between the two objectives in real system, respectively. There are a large number of networks in the real world, such as Internet networks, social networks, biological networks, railway network and so on. As many ecological and epidemiological processes take place on network structures, more and more scholars in the field pay attention to complex networks, which mainly include three research contents: (1) the statistical characteristics

of real networks, such as degree distribution, clustering coefficient, path lengths, degree correlation, etc [1, 2, 3, 4]; (2) evolution dynamics of the topological structure of networks [5, 6, 7, 8]; (3) the topological structures of coupled networks, such as multi-layer networks, metapopulation networks, hyper-networks [9, 10, 11, 12, 13].

Since ancient times, infectious diseases have been frequently prevalent in human society, which seriously endangered human health, life and social development process [14, 15, 16, 17]. Therefore, to study the spread of infectious diseases in the population, various infectious disease models are established and analyzed, the research output provide theoretical bases for the prevention and control of infectious diseases [18, 19, 20, 21, 22]. The classical epidemic transmission models usually assume that the population is uniformly mixed, that is, the probability of contact between any two individuals in the population is same, this is not true in the real world scenarios. In order to describe realistic disease transmission, it is essential to study the spread of epidemic through the networks. Klov Dahl and May combined social networks with epidemiology to study the spread of HIV in the population [23, 24]. The SIR model with repeated contacts between the same individuals on regular networks was considered by Diekmann et al. [25]. Moreno et al. gave the critical threshold of the SIR-type epidemics on degree distribution with exponential distribution [26]. Volz made use of the probability generating function to study SIR dynamical model on random networks [27]. Bauch used moment closure methods to calculate the basic reproductive number of an SIS epidemic network model [28]. Moore and Newman constructed epidemic model on small-world networks, then calculated critical threshold of epidemic spread [29]. The absence of an epidemic threshold and its associated critical behavior on a wide range of scale-free networks are confirmed by Pastor-Satorras and Vespignani [30].

Over the past decades, many scholars investigated how the topological structure of the network affected the dynamics of disease transmission, while they ignore that the influence of the spread of infectious disease on the structure of network. For example, during SARS outbreak, the flights into Hong Kong were found to be 80% lower than usual situations due to the changes of people's behavior caused by SARS epidemic in Hong Kong [31]. In fact, the individuals take some measures to protect themselves from infection in face of the outbreaks of infectious diseases, such as vaccination, wearing a mask, avoiding going to public places, cutting off contact with infected individuals, etc. The alternation of the individuals' behavior caused by diseases has great effects on the structure of network, which in turn affect the spread process of infectious diseases. Individuals adjust their behavior based on the prevalence situations of the current disease, namely adaptive behavior in the spread of infectious disease on networks, which is described by link disconnection and rewiring based on the disease status of the population [32, 33, 34, 35, 36]. Gross et al. firstly introduced the mechanism of individuals' adaptive changes in their behavior with assumption that, in order to reduce the infection risk, the susceptible individuals cut off the connections with the infected neighbors and immediately rewire other susceptible individuals [32]. Zanette and Risau-Gusmão studied that the susceptible agents break the links with the infected agents and rewire to the rest of population with certain probability, they further indicated that an appropriate rewiring probability is able to suppress the spread of infectious diseases [33]. Szabó-Solticzky et al. gave an adaptive mechanism that non-existing links are activated and existing links are deleted with different rates [35]. In addition, other rewiring mechanisms in network epidemic models was proposed in recent years [37, 38, 39].

In reality, during the process of adaptive changes of individuals' behavior, the alternative action of changes normally do not occur immediately, but take some time to respond, thus we need to consider

the factor of time taken in such process. Therefore, based on the mechanism of adaptive changes of individuals' behavior proposed by Gross et al. [32], we introduce time delay in rewiring process, namely the susceptible individuals need take a period of time to search for other susceptible persons and go to rewire. By theoretical analysis, we find that, with such rewiring time, the delayed SIS network model with adaptive rewiring is quite different from usual delayed model, the long-term steady states may lie on a line in a high-dimensional state space where the mathematical foundation for its deep dynamical analysis is lacked. However, from the numerical viewpoint, we can find that the introduction of rewiring time can greatly impact on the transmission dynamics of infectious disease. As expected, increasing the rewiring time leads to a suppression in the size of infected population and higher probability of smaller outbreaks. Our results indicates that once the susceptible persons disconnect the connections with infected individuals, better to wait some time before creating new connections with the healthy ones, such strategy has potential influence on disease control.

This article is organized as follows: In Section 2, we establish a delayed SIS network model with adaptive rewiring mechanism. The long-term steady states for the system with and without the rewiring delay are analyzed in section 3, we have found that there are at most three equilibria when the system has no rewiring time, while the equilibria of the system with rewiring delay lie on a line in a four-dimensional state space. In Section 4, the numerical simulation results show the significant differences of the dynamical behavior in the system with or without rewiring time, implying that the introduction of rewiring time promotes obvious effect on controlling disease transmission. Conclusions and discussions are drawn in Section 5.

## 2. Model formation

During a disease outbreak, once the healthy individuals recognize the infection risk in disease transmission process, instinctively they incline to protect themselves by cutting off connection with infected individuals, which is so called individuals' adaptive behavior in the spread of infectious disease on contact network, resulting in the alteration of the topological structure in the network, an example given in Figure 1.

To discuss such situation, Gross et al. firstly put forward a mechanism of adaptive behavior by link-breaking and link-creating, that is, the susceptible individuals disconnect the links with the infected persons and immediately rewire other susceptible ones [32], and introduced the notations  $X, Y, Z \in \{S, I\}$  for the state of each node,  $[X]$ ,  $[XY]$ ,  $[XYZ]$  for the number of nodes in state  $X$ , links in states  $X - Y$  and triples in states  $X - Y - Z$  respectively, here the pairs are counted once in each direction (namely  $[XY] = [YX]$ ) and  $[XX]$  is counted twice, and considered a susceptible-infected-susceptible (SIS) epidemic model on such network with a constant number of nodes  $N$ ,

$$\begin{aligned}
 [\dot{S}] &= -\beta[S I](t) + \gamma[I](t), \\
 [\dot{I}] &= \beta[S I](t) - \gamma[I](t), \\
 [\dot{S S}] &= -2\beta[S S I](t) + 2\gamma[S I](t) + 2\omega[S I](t), \\
 [\dot{S I}] &= \beta([S S I](t) - [I S I](t) - [S I](t)) - \gamma[S I](t) + \gamma[I I](t) - \omega[S I](t), \\
 [\dot{I I}] &= 2\beta([I S I](t) + [S I](t)) - 2\gamma[I I](t),
 \end{aligned} \tag{2.1}$$

where susceptible individuals are infected by their infected neighbors at a transmission rate  $\beta$  in each

$S - I$  link,  $\gamma$  is the recovery rate of the infected individuals. The susceptible individual breaks the link with infected one ( $S - I$ ) at rewiring rate  $\omega$  and immediately rewiring other susceptible individuals with the same rate  $\omega$ . More specifically, the states of two nodes in a link may change: any susceptible node in the  $S - S$  link can be infected by its neighbor in a  $S - S - I$  triples (represented by  $\beta[S S I]$ ), which converts  $S - S$  link into  $S - I$  link; similarly,  $S - I$  link turns into  $I - I$  link due to the susceptible node in the  $S - I$  link infected by the infected node in  $S - I$  link ( $\beta[S I I]$ ) or another infected neighbor in  $I - S - I$  triple ( $\beta[I S I]$ ). The recovery of the infected node in  $S - I$  link results in  $S - S$  link ( $\gamma[S I]$ ); either of two infected nodes in  $I - I$  link can recover yielding  $S - I$  link ( $\gamma[I I]$ ).

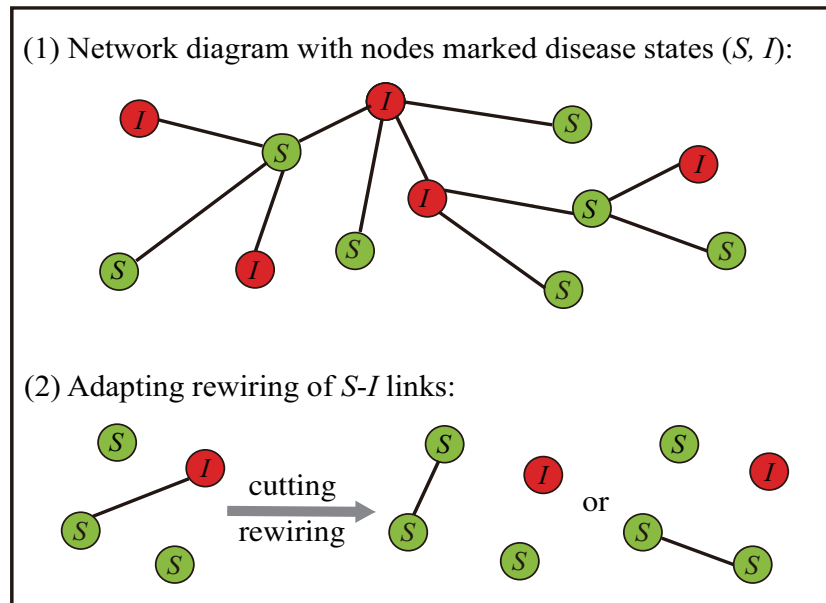


Figure 1. (1) The structure diagram of undirected network with nodes and links, where the disease states of nodes are marked as susceptible ( $S$ ) or infected ( $I$ ); (2) the adaptive rewiring of  $S - I$  links, that is, susceptible node in  $S - I$  link cut off the connection with infected neighbors and randomly rewired other susceptible nodes.

Based on the above SIS network model with adaptive rewiring given in Gross[32], we introduce rewiring delay in such reconnection process, and consider the case that once the susceptible individuals realize the infection possibility from their connected infectious neighbors, they break such connections and take time  $\tau$  to look for other susceptible individuals to rewire. In order to close system, assuming that in the triple links  $[XYZ]$ , the numbers of neighbors of  $Y$ -state node on the network follows Poisson distribution [40], i.e.,  $[XYZ] = \frac{[XY][YZ]}{[Y]}$ . By incorporating time delay and the special triple links into the model (2.1), we can obtain the following delayed SIS network model with adaptive rewiring:

$$\begin{aligned}
 [\dot{S}](t) &= -\beta[S I](t) + \gamma[I](t), \\
 [\dot{I}](t) &= \beta[S I](t) - \gamma[I](t), \\
 [S' S](t) &= -2\beta \frac{[S S](t)[S I](t)}{[S](t)} + 2\gamma[S I](t) + 2\omega[S I](t - \tau), \\
 [S I](t) &= \beta \left( \frac{[S S](t)[S I](t)}{[S](t)} - \frac{[S I](t)[S I](t)}{[S](t)} - [S I](t) \right) - \gamma[S I](t) + \gamma[I I](t) - \omega[S I](t), \\
 [I I](t) &= 2\beta \left( \frac{[S I](t)[S I](t)}{[S](t)} + [S I](t) \right) - 2\gamma[I I](t).
 \end{aligned} \tag{2.2}$$

In this work, we do not consider the demographic factor in the network connection, so the number of total nodes

$$N = [S](t) + [I](t) \quad (2.3)$$

is a constant from  $[\dot{S}](t) + [\dot{I}](t) = 0$ . Consequently, the system (2.2) can be reduced to:

$$\begin{aligned} [\dot{I}](t) &= \beta[S I](t) - \gamma[I](t), \\ [S\dot{S}](t) &= 2\left(-\beta\frac{[S S](t)}{N - [I](t)} + \gamma\right)[S I](t) + 2\omega[S I](t - \tau), \\ [S\dot{I}](t) &= \left(\beta\frac{[S S](t)}{N - [I](t)} - \beta\frac{[S I](t)}{N - [I](t)} - \beta - \gamma - \omega\right)[S I](t) + \gamma[II](t), \\ [I\dot{I}](t) &= 2\beta\left(\frac{[S I](t)}{N - [I](t)} + 1\right)[S I](t) - 2\gamma[II](t). \end{aligned} \quad (2.4)$$

In order to simplify the notions, let

$$u_1 = [I], \quad u_2 = [S S], \quad u_3 = [S I], \quad u_4 = [II], \quad (2.5)$$

model (2.4) becomes:

$$\begin{aligned} \dot{u}_1(t) &= \beta u_3(t) - \gamma u_1(t), \\ \dot{u}_2(t) &= 2\left(-\beta\frac{u_2(t)}{N - u_1(t)} + \gamma\right)u_3(t) + 2\omega u_3(t - \tau), \\ \dot{u}_3(t) &= \left(\beta\frac{u_2(t)}{N - u_1(t)} - \beta\frac{u_3(t)}{N - u_1(t)} - \beta - \gamma - \omega\right)u_3(t) + \gamma u_4(t), \\ \dot{u}_4(t) &= 2\beta\left(\frac{u_3(t)}{N - u_1(t)} + 1\right)u_3(t) - 2\gamma u_4(t). \end{aligned} \quad (2.6)$$

In the following, we mainly work on the model (2.6) from the point of view of dynamics analysis.

### 3. Mathematical analysis

To discuss the dynamical behavior of system (2.6) and the effect of rewiring delay  $\tau$ , we investigate the system without and with delay first.

If the rewiring time  $\tau = 0$ , that means, when the susceptible individuals cut off the connection with the infected person, they rewire the other susceptible ones immediately. For such case, from  $\dot{u}_2(t) + 2\dot{u}_3(t) + \dot{u}_4(t) = 0$ , we have  $u_2(t) + 2u_3(t) + u_4(t) = nN$ , where  $n$  is the average degree of the network, so the system (2.6) can be further reduced to

$$\begin{aligned} \dot{u}_1(t) &= \beta u_3(t) - \gamma u_1(t), \\ \dot{u}_2(t) &= 2\left(-\beta\frac{u_2(t)}{N - u_1(t)} + \gamma\right)u_3(t) + 2\omega u_3(t), \\ \dot{u}_3(t) &= \left(\beta\frac{u_2(t)}{N - u_1(t)} - \beta\frac{u_3(t)}{N - u_1(t)} - \beta - \gamma - \omega\right)u_3(t) + \gamma(nN - u_2(t) - 2u_3(t)), \end{aligned} \quad (3.1)$$

which is studied in [32] numerically. From dynamical point of view, we can see that, in system (3.1), there is a disease-free equilibrium  $E_0 = (0, nN, 0)$  and up to two endemic equilibria  $(u_1^*, u_2^*, u_3^*)$  with  $u_1^*$  satisfying the following quadratic equation:

$$(\beta - \omega)(u_1^*)^2 - (n\beta + \beta - 2\omega)Nu_1^* + (n\beta - \gamma - \omega)N^2 = 0. \quad (3.2)$$

More specifically,

Case 1: when  $C_1 := \omega - \beta = 0$ . If  $C_2 := n\beta - \beta - \gamma > 0$ , we have unique  $u_1^* = \frac{n\beta - \beta - \gamma}{n\beta - \beta}N = (1 - \frac{\gamma}{n\beta - \beta})N$  with  $0 < u_1^* < N$ . Thus there exists a unique endemic equilibrium  $E_s = (u_1^*, u_2^*, u_3^*)$  in the system (3.1) with  $u_2^*, u_3^*$  determined in the following (3.3):

$$u_2^* = \frac{(\gamma + \omega)(N - u_1^*)}{\beta}, \quad u_3^* = \frac{\gamma u_1^*}{\beta}. \quad (3.3)$$

Otherwise there is no endemic equilibrium.

Case 2: if  $C_1 = \omega - \beta \neq 0$ . From Eq. (3.2), we can obtain:

$$u_{1\pm}^* = \frac{1}{2} \frac{(\beta n + \beta - 2\omega \pm \sqrt{\Delta})N}{\beta - \omega},$$

where  $\Delta = (\beta n + \beta - 2\omega)^2 - 4(\beta - \omega)(n\beta - \gamma - \omega) = (n - 1)^2\beta^2 + 4\gamma(\beta - \omega)$ .

Depending on the parameters, we have more subcases for either (i)  $C_1 < 0$  and (ii)  $C_1 > 0$ .

i): when  $C_1 < 0$ ,

a) with  $C_3 = n\beta - \gamma - \omega > 0$ ,  $\Delta < (\beta n + \beta - 2\omega)^2$  is obvious and  $\beta n + \beta - 2\omega \geq 2(\beta - \omega) > 0$ , therefore  $u_{1\pm}^* > 0$ . In addition,

$$u_{1\pm}^* = \frac{1}{2} \frac{(\beta n + \beta - 2\omega \pm \sqrt{\Delta})N}{\beta - \omega} \geq \frac{1}{2} \frac{(2(\beta - \omega) \pm \sqrt{\Delta})N}{\beta - \omega} = N \pm \frac{1}{2} \frac{N\sqrt{\Delta}}{\beta - \omega},$$

we have  $u_{1-}^* < N$ ,  $u_{1+}^* > N$  which is impossible since  $N$  is the total number of the population. Thus for this subcase, there is only unique feasible positive equilibrium  $E_1 = (u_{1-}^*, u_{2-}^*, u_{3-}^*)$  in (3.1) as well.

b) with  $C_3 = 0$ , we have  $u_{1-}^* = 0$ ,  $u_{1+}^* = \frac{1}{2} \frac{2(\beta n + \beta - 2\omega)N}{\beta - \omega} \geq \frac{2(\beta - \omega)N}{\beta - \omega} = 2N$ , so there is no positive equilibrium existed in the system (3.1).

c) if  $C_3 < 0$ , first, we have  $u_{1-}^* < 0$ ,  $u_{1+}^* > 0$  and further we can obtain that  $u_{1+}^* > \frac{1}{2} \frac{2(\beta n + \beta - 2\omega)N}{\beta - \omega} \geq \frac{2(\beta - \omega)N}{\beta - \omega} = 2N$  which is contradict to (2.3). Again, no any positive equilibrium in the system (3.1).

Similarly, we can discuss the subcase for (ii)  $C_1 > 0$ . We can see that:

a) when  $C_3 > 0$ ,  $0 < u_{1-}^* < N$ ,  $u_{1+}^* < 0$ , then system (3.1) has a unique positive equilibrium  $E_1 = (u_{1-}^*, u_{2-}^*, u_{3-}^*)$ ;

b) when  $C_3 = 0$  and  $C_4 = n\beta + \beta - 2\omega < 0$ , there is a unique positive equilibrium  $E_1 = (u_{1-}^*, u_{2-}^*, u_{3-}^*)$ ;

c) while if  $C_3 < 0$ ,  $C_4 = n\beta + \beta - 2\omega < 0$  and  $\Delta > 0$ , there are two endemic equilibria  $E_1 = (u_{1-}^*, u_{2-}^*, u_{3-}^*)$  and  $E_2 = (u_{1+}^*, u_{2+}^*, u_{3+}^*)$  with

$$u_{1-}^* < \frac{1}{2} \frac{(\beta n + \beta - 2\omega - (n - 1)\beta)N}{\beta - \omega} = \frac{1}{2} \frac{2(\beta - \omega)N}{\beta - \omega} = N,$$

$$u_{1+}^* \leq \frac{1}{2} \frac{(2(\beta - \omega) + \sqrt{\Delta})N}{\beta - \omega} = N + \frac{1}{2} \frac{\sqrt{\Delta}N}{\beta - \omega} < N,$$

No. E.E	Conditions
None	$C_1 = 0, C_2 \leq 0$ ; or $C_1 < 0, C_3 \leq 0$
$E_s/E_1$	$C_1 = 0, C_2 > 0$ ; or $C_1 < 0, C_3 > 0$ ; or $C_1 > 0, C_3 > 0$ ; or $C_1 > 0, C_3 = 0, C_4 < 0$
$E_1, E_2$	$C_1 > 0, C_3 < 0, C_4 < 0, \Delta > 0^*$

**Table 1.** Conditions for existence of endemic equilibria(E.E) \* In addition, if  $\Delta = 0$ , then  $E_1 = E_2$

when  $\Delta = 0$ , we can get  $u_{1-}^* = u_{1+}^*$ , which indicates that  $E_1$  and  $E_2$  coincide.

Summarizing the above analysis, we can provide the conditions for the existence of none, one or two endemic equilibria in the simplified system (3.1) without rewiring delay.

The stability of each endemic equilibrium has been studied in [41] through some nonlinear transformation, and the authors claimed theoretically that the adaptive epidemic model exhibited rich dynamic behaviors, including backward bifurcation, saddle-node bifurcation, Hopf bifurcation, homoclinic bifurcation and Bogdanov-Takens bifurcation of codimension 2, and further confirmed some of the phenomena shown in [32] numerically. Therefore, the interplay between the adaptive changes of individual behavior and the topological structure of network have profound influence on the spread of network epidemic.

With the rewiring time  $\tau > 0$ , different from most of the dynamical systems, it is interesting for us to find that, instead of the existence of finite steady states or equilibria, in the system (2.6), there are infinite equilibria sitting on a line  $L$  and they are independent of the value of  $\tau$ , represented by:

$$L = \left\{ 0 \leq u_1 < N, u_2 = \frac{(\gamma + \omega)(N - u_1)}{\beta}, u_3 = \frac{\gamma}{\beta} u_1, u_4 = \frac{(N\beta - \beta u_1 + \gamma u_1)u_1}{\beta(N - u_1)} \right\}$$

and each equilibrium on line  $L$  is a function of  $u_1$ , implying that, from (2.5), with the constant parameters, the number of infected population determines the size of each link of  $[SS]$ ,  $[SI]$  and  $[II]$  on the network.

In particular, when  $u_1 = 0$ , the disease-free equilibrium in (2.6) is  $E_0^\tau(0, \frac{(\gamma + \omega)N}{\beta}, 0, 0)$ , which is different from  $E_0(0, nN, 0)$  in system (3.1), due to the fact that, with rewiring time, the process leads to the number of the total edges of the network is no longer  $nN$ . When the infected number is getting to sufficient small, there is only the connection among the susceptible individuals on network, which is related to the recovery, rewiring and infection rates.

One can further derive the characteristic equation at  $E_0^\tau$ ,

$$\lambda^2(\lambda + \gamma)(\lambda + 2\gamma + \beta) = 0. \quad (3.4)$$

It is obvious that beside two eigenvalues  $\lambda = -\gamma$  and  $\lambda = -(2\gamma + \beta)$ , there are two zero eigenvalues which are independent of any system parameters. Thus the stability of  $E_0^\tau$  is governed by the dynamical behavior in a 2-dimensional center manifold. Different from Bogdanov-Takens bifurcation, this bifurcation is highly degenerated. This is a challenging research topic in functional differential equations, we leave it as future research.

Consequently, it is not trivial to analyze the local stability of each equilibrium on the line  $L$ , although we can still linearize system (2.6) at each equilibrium  $(u_1^*, u_2^*, u_3^*, u_4^*)$ , that is:

$$\begin{aligned} \dot{u}_1(t) &= -\gamma u_1(t) + \beta u_3(t), \\ \dot{u}_2(t) &= -\frac{2(\gamma + \omega)\gamma u_1^*}{\beta(N - u_1^*)} u_1(t) - \frac{2\gamma u_1^*}{N - u_1^*} u_2(t) - 2\omega u_3(t) + 2\omega u_3(t - \tau), \\ \dot{u}_3(t) &= \frac{(N\gamma + N\omega - 2\gamma u_1^* - \omega u_1^*)\gamma u_1^*}{\beta(N - u_1^*)^2} u_1(t) + \frac{\gamma u_1^*}{N - u_1^*} u_2(t) - \frac{N\beta - \beta u_1^* + 2\gamma u_1}{N - u_1^*} u_3(t) \\ &\quad + \gamma u_4(t), \\ \dot{u}_4(t) &= \frac{2\gamma^2 (u_1^*)^2}{\beta(N - u_1^*)^2} u_1(t) + \frac{2(N\beta - \beta u_1^* + 2\gamma u_1^*)}{N - u_1^*} u_3(t) - 2\gamma u_4(t), \end{aligned} \quad (3.5)$$

then the corresponding characteristic equation can be derived as:

$$\Delta(\lambda) = \lambda^4 + a_3\lambda^3 + a_2\lambda^2 + a_1\lambda + a_0 + (b_2\lambda^2 + b_1\lambda + b_0)e^{-\lambda\tau} = 0, \quad (3.6)$$

where

$$\begin{aligned} a_3 &= \frac{(N - u_1^*)\beta + 3N\gamma + \gamma u_1^*}{(N - u_1^*)} > 0, \\ a_2 &= \frac{\gamma(N^2\beta + 2N^2\gamma + 3N\gamma u_1^* + N\omega u_1^* - \beta(u_1^*)^2 - \omega(u_1^*)^2)}{(N - u_1^*)^2} = \frac{\gamma(\beta(N^2 - (u_1^*)^2) + 2N^2\gamma + 3N\gamma u_1^* + \omega u_1^*(N - u_1^*))}{(N - u_1^*)^2} > 0 \\ a_1 &= \frac{2\gamma^2 u_1^*(N^2\beta + N^2\gamma + 2N^2\omega - 2N\beta u_1^* - 4N\omega u_1^* + \beta(u_1^*)^2 + 2\omega(u_1^*)^2)}{(N - u_1^*)^3} > 0, \\ a_0 &= \frac{4\gamma^3 \omega u_1^*}{N - u_1^*} > 0, \\ b_2 &= \frac{-2\gamma \omega u_1^*}{N - u_1^*} < 0, \\ b_1 &= \frac{-6\gamma^2 \omega u_1^*}{N - u_1^*} < 0, \\ b_0 &= -\frac{4\gamma^3 \omega u_1^*}{N - u_1^*} < 0. \end{aligned}$$

It is obvious that the local stability of equilibrium also depends on  $u_1^*$ . The difficulty is that we cannot use the normal method to analyze the distribution of the roots in the characteristic equation (3.6). Even it can be done numerically, to the best of our knowledge, there is no method yet to investigate their stability since the introduction of rewiring delay  $\tau$  gives rise to infinite equilibria.

The existence of line equilibria is a surprising dynamical feature which is rarely found in normal dynamical systems, let alone the theoretical analysis. Through the literature review, we know that, the line equilibria in a simple SIR model without time delay was discussed in [42, 43] where 2-dimensional global center manifold is introduced to understand the global dynamical properties of the system. In [42, 43], Li et al. gave the local stability of each equilibrium on line by analyzing the eigenvalues and the corresponding eigenvectors, and further proved a 2-dimensional global center manifold which consist of heteroclinic orbits connecting a pair of equilibria on line. With respect to our model (2.6) with time delay and four state variables, we can not provide deep theoretical analysis at this stage, instead, we investigate the rich dynamics by numerical simulations. Next, we will mainly explore and compare the system with and without rewiring delay.



#### 4. Numerical simulations

To verify the different dynamical behavior for the model without and with the rewiring delay numerically, we adopt some parameter values from the literature [32, 36] and choose three sets of parameters corresponding to different number of equilibria in Table 1 to do the simulations.

First we choose the parameter values

$$N = 1000, n = 2, \gamma = 0.03, \text{ and } \beta = \omega = 0.06. \quad (4.1)$$

When the rewiring takes place without waiting time, i.e.  $\tau = 0$ , we have  $C_1 = 0, C_2 > 0$  in Table 1, then there is a unique positive equilibrium  $E_s = (500, 750, 250)$  in system (3.1) (See the red point in Figure 2(f)). Numerical result (Figure 2(a)) shows  $E_s$  is locally asymptotically stable. With certain rewiring time, i.e.  $\tau \neq 0$ , we understand that there are infinite steady states which lie on the line  $L$  (See the black line in Figure 2(f)). To test the variation of number in infected individuals ( $[I](t)$ ) and the links between susceptible group ( $[SS](t)$ ), with respect to the rewiring time  $\tau$ , we increase the value of  $\tau$  gradually to a critical threshold  $\tau^*$ . With the fixed parameter values given in (4.1), we have  $220 < \tau^* < 230$ . We can find that under the same initial condition  $I_0$ , the long-term dynamical behavior is similar, in the sense that, it approaches to a steady state on the line  $L$  which is drawn in Figure 2(b)-(e), but with different strengths, that is, different points on  $L$  which are the green points  $P_i, i = 1, 2, 3, 4$  in Figure 2(f). While when the rewiring time crosses the threshold  $\tau^*$ , we can observe the periodically oscillatory behavior which are drawn in Figure 3, where Figure 3(a),(c) represent the time histories and the limit cycles are confirmed in the three dimensional phase space (see Figure 3(b),(d)), where the black line  $L$  represents the equilibria line and the red closed circle is the stable limit cycle centered at an equilibrium at  $L$ .

It is interesting to find, from Figures 2 and 3, that (i) with short rewiring time, the infected population ( $[I]$ ) and their associated links ( $[SI]$ ) increases at beginning, then reach the steady states gradually, in opposite with the decreasing of the links between the susceptible population ( $[SS]$ ). When the rewiring time is closing to the critical value  $\tau^*$ , the trajectories of each state become oscillatory decay to a steady state; (ii) with rewiring time, depending on the location of the initial condition (left or right w.r.t.  $E_s$ ), the system approaches to certain steady state on the left or right of the steady state  $E_s$  which is associated to instant rewiring respectively; (iii) with the increase of  $\tau$  after crossing to the critical value (i.e.  $\tau > \tau^*$ ), this oscillation becomes more strong, in the sense that, the steady state loss the stability with the increasing amplitudes and slower frequencies. Finally the orbits approach to the stable limit cycle.

To check the existence of two positive equilibria in system (3.1) when there is no rewiring time, we fix  $N = 1000, n = 20, \beta = 0.003, \gamma = 0.002$  and  $\omega = 0.23 \neq \beta$ , the condition  $C_1 > 0, C_3 < 0, C_4 < 0, \Delta > 0$  in Table 1 holds, we can obtain two endemic steady states  $E_1 = (957.8, 3261.1, 638.6)$  and  $E_2 = (791.1, 16157, 527.4)$  by numerical simulations. By choosing the initial condition closing to these two endemic states, Figure 4(a) shows that all the trajectories approach to the disease-free equilibrium  $E_0$  and are away from  $E_1$  and  $E_2$ , implying that both  $E_1, E_2$  are unstable, but  $E_0$  is stable. In Figure 4(a) we specify a green curve showing the solution trajectory from initial value  $I_0 = (700, 1000, 9000, 1000)$  which is used to do the comparison with different  $\tau$ . While with the rewiring time  $\tau \neq 0$ , system (2.6) has infinite equilibria on the line  $L$  (see Figure 2(f)). With the increase of  $\tau$ , Figure 4(b)-(e) present the similar long-term dynamical behavior under the same initial condition  $I_0$ . We can see that the numbers of the infected population  $[I](t)$  and  $[SS](t)/[SI](t)$  links eventually approach to steady

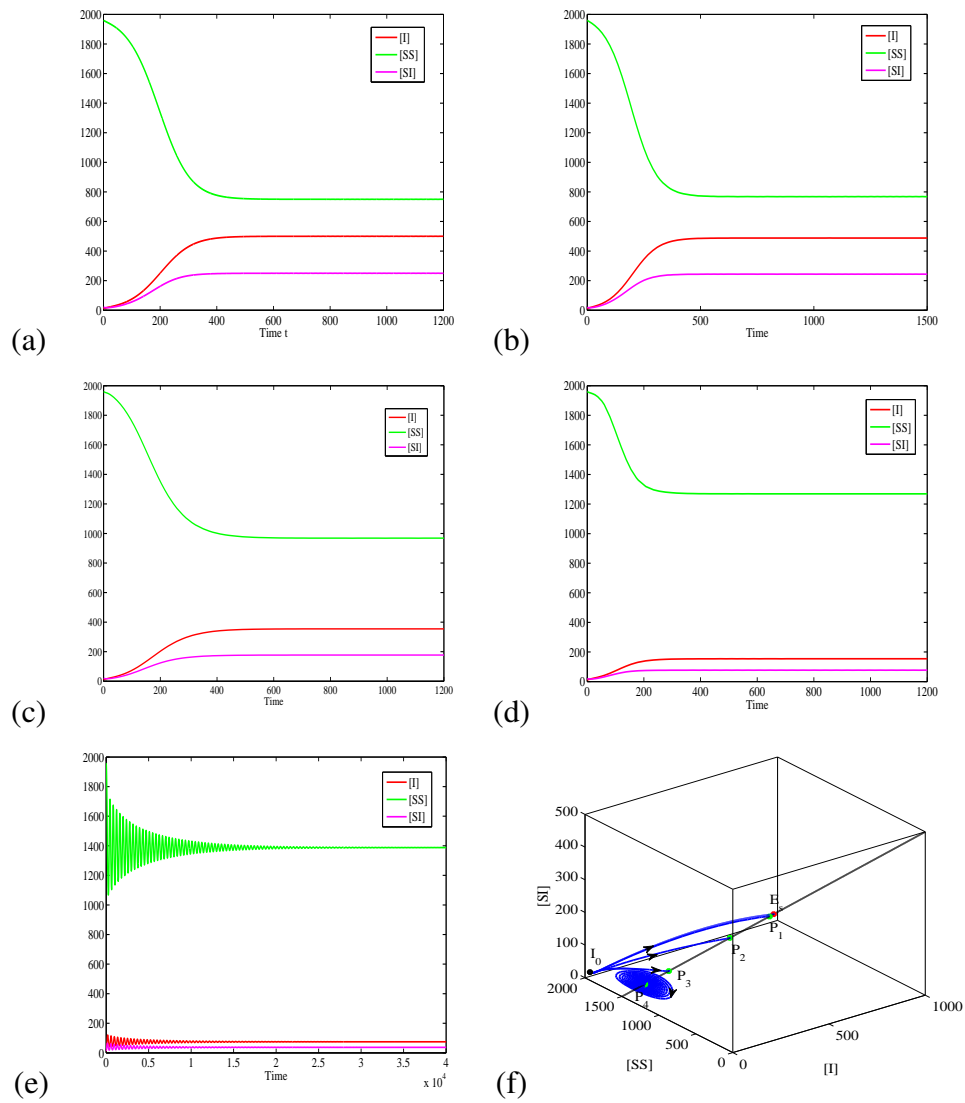


**Figure 2.** With different rewiring delay: (a)  $\tau = 0$ , showing  $E_s$  is stable; (b)-(e) with  $\tau = 1, 12, 60, 220$ , showing the trajectory approaches to a point  $P_1, P_2, P_3$  and  $P_4$  on  $L$  in (f) respectively.

states  $P_i, i = 1, 2, 3$  (green dots) on the line  $L$  (see Figure 4(g)), but the time evolutions is different at beginning: the infected population  $[I](t)$  gradually increases;  $[SS](t)$  links increase to a high peak value, then decrease rapidly;  $[SI](t)$  links decreases in the form of oscillatory decay. The possible reason is that high rewiring rate  $\omega$  leads to the in the number of  $S - I$  links and the increase of  $S - S$  links simultaneously, which further leads to the entire network separated into two connected clusters of noninfected and infected groups. These two clusters are connected through  $S - I$ . As the spread of infectious disease reduces,  $S - I$  links further decreases, so the number of reconnected  $S - S$  links decrease. Figure 4(f) presents the solution trajectories, from the same initial value  $I_0$ , approach to different steady state on line  $L$  for different rewiring time. In order to observe the final approach of the trajectories for different  $\tau$  (green dots in Figure 4(f)) more clear, we intercept and enlarge the part of Figure 4(f) in Figure 4(g).

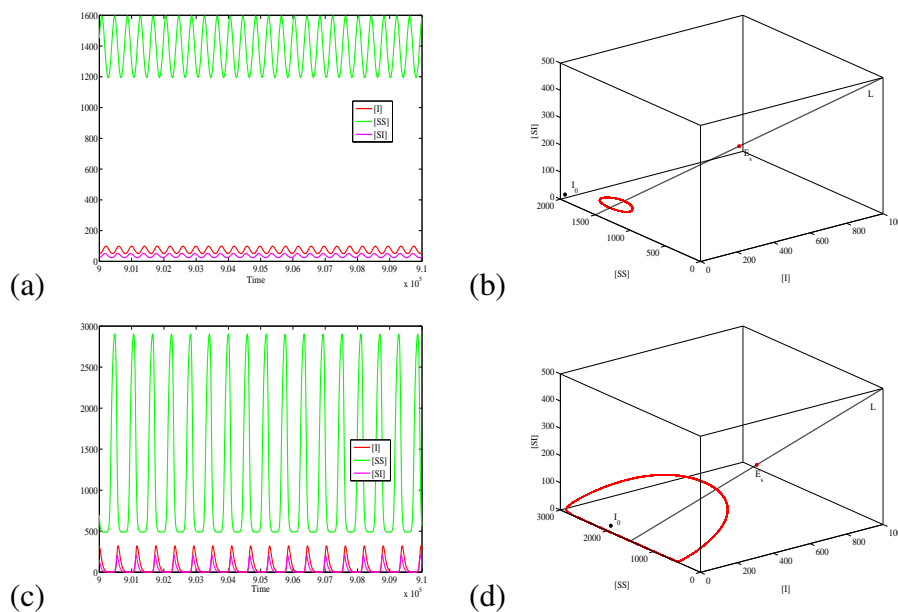


**Figure 3.** Long-term oscillatory behavior and phase portraits with different  $\tau$ . (a)(b)  $\tau = 230$ ; (c)(d)  $\tau = 389$ .

With other parameter choice, e.g.,  $N = 1000$ ,  $n = 10$ ,  $\beta = 0.003$ ,  $\gamma = 0.005$ ,  $\omega = 0.03 \neq \beta$  and  $\tau = 0$ , the condition  $C_1 > 0$ ,  $C_3 < 0$ ,  $C_4 < 0$ ,  $\Delta > 0$  is also satisfied in Table 1, we can still obtain two positive equilibria  $E_1 = (754.6, 2863.1, 1257.6)$  and  $E_2 = (245.4, 8803.5, 409.0)$ . Different from the case in Figure 4, we can observe that  $E_1$  and  $E_0$  are stable, but  $E_2$  is unstable (see Figure 5(a) and (b)). This indicates that under these parameters, bistable phenomenon occur in system (3.1). The green curve in Figure 5(a) is the solution trajectory from initial value  $I_0 = (10, 2000, 300, 7400)$ . Based on this initial value  $I_0$ , next, we present the time evolutions of numbers of the infected nodes  $[I](t)$  and  $[SS](t)/[SI](t)$  links by increasing the value of  $\tau$  gradually to a critical threshold  $\tau^*$  with  $400 < \tau^* < 418$ . The long-term dynamical behavior of system (2.6) is given in Figure 5(c)-(g) with different value of  $\tau$ , namely eventually approach to certain steady state  $P_i, i = 1, 2, 3, 4$  (the green dots in Figure 5(g)). Finally when the rewiring time crosses the threshold  $\tau^*$ , similar to the case shown in Figure 3, we can observe the periodically oscillatory behavior and stable limit cycle (See Figure 6).

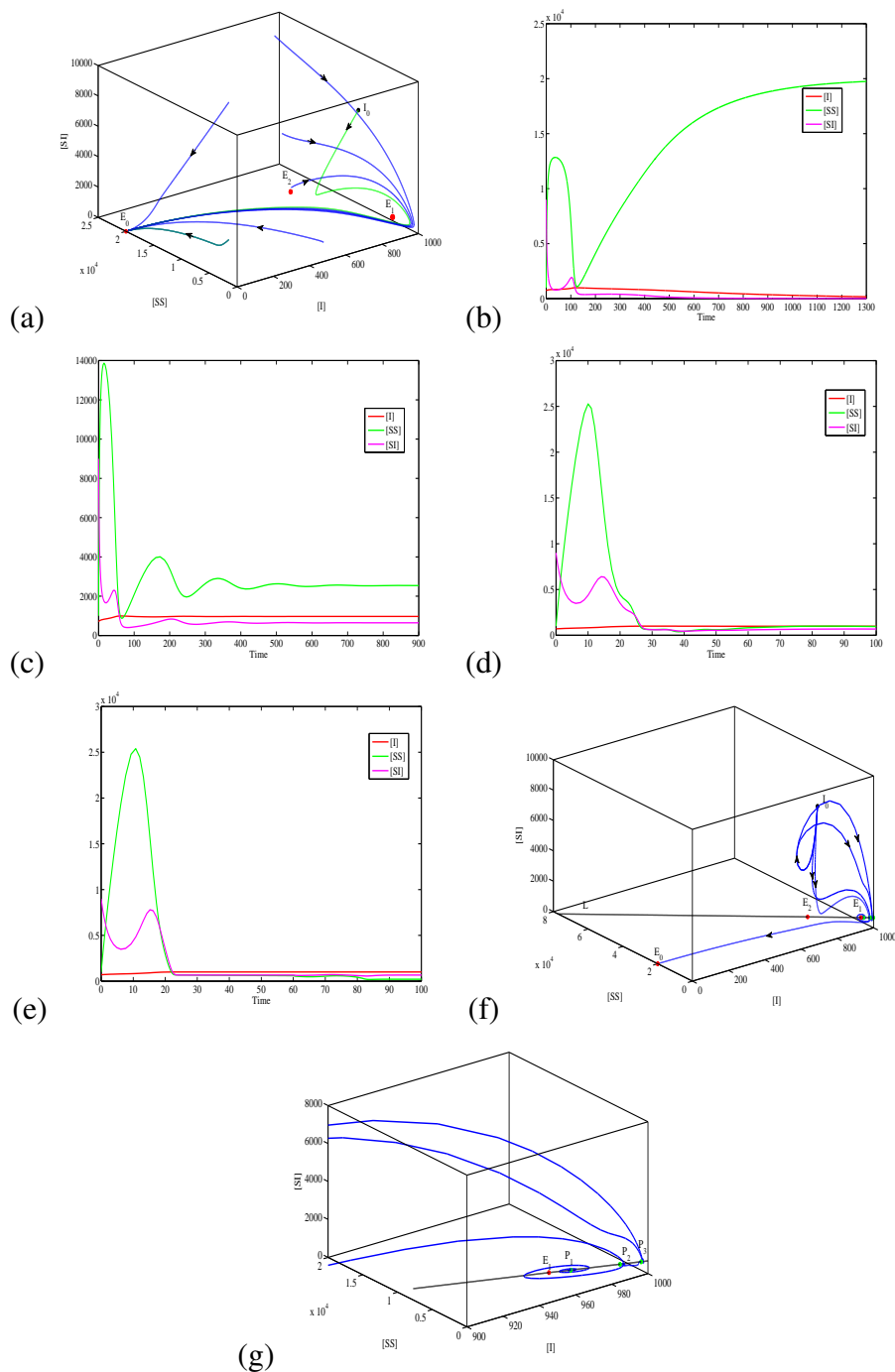


**Figure 4.** (a) the stabilities of  $E_0$ ,  $E_1$  and  $E_2$  are shown by the phase diagram for  $\tau = 0$ ; (b) showing  $E_0$  is stable with  $\tau = 0$ ; With different rewiring delay:  $\tau = 1, 10, 60$ , (c)-(e) shows the trajectory approaches to a point  $P_1, P_2$  and  $P_3$  on  $L$  in (f) respectively. (g) is an enlarged part of (f).

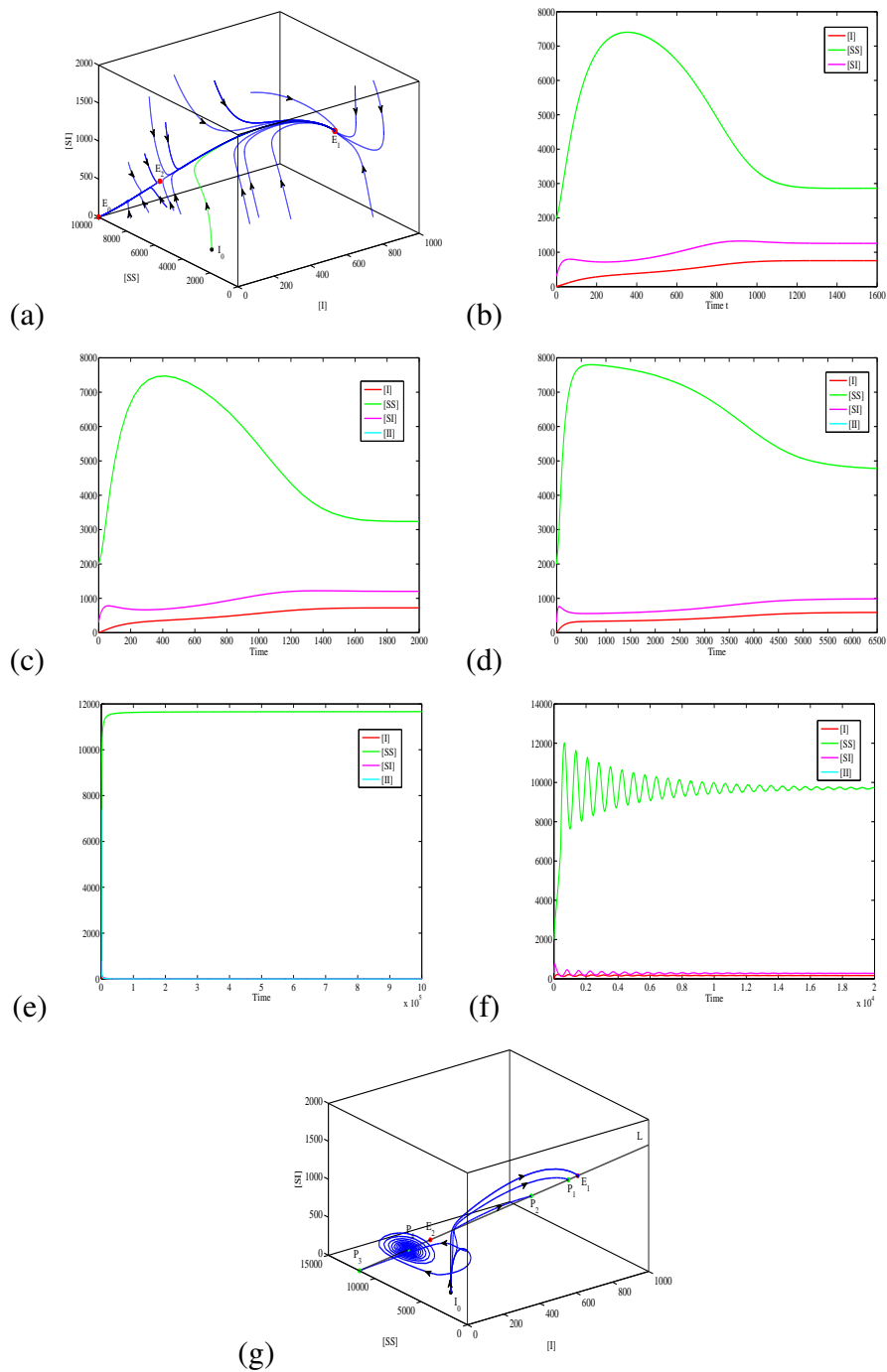


**Figure 5.** (a) The bistable phenomenon of system (3.1) is shown by phase portrait. (b)  $E_1$  is stable when  $\tau = 0$ ; With different rewiring delay:  $\tau = 10, 30, 92, 400$ , (c)-(f) shows the trajectory approaches to a point  $P_1, P_2, P_3$  and  $P_4$  in (g) respectively.

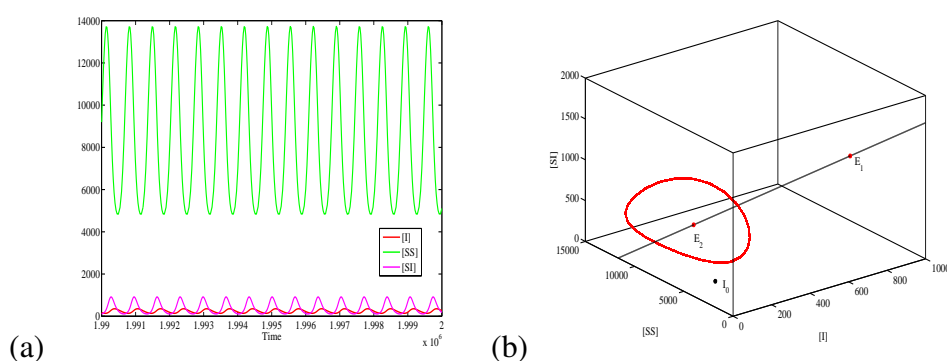


**Figure 6.** Long-term oscillatory behavior and phase portraits with rewiring delay  $\tau = 418$ .

## 5. Conclusions and discussions

In the face of the outbreak of infectious disease, people tend to protect themselves from the transmission of infectious disease by adjusting their behavior, such as cutting off links with infected neighbors and rewiring with other healthy individuals. In order to better describe the situation that after breaking the connection with infected person, the susceptible individuals need to take time to look for the other susceptible persons to rewire, we thus introduce delay in rewiring process and establish a delayed SIS network model with adaptive rewiring. By theoretical analysis, we find a novel result that, in the system, there are infinite equilibria which lie on a line in a high-dimensional state space, which is rarely existed in the dynamical systems of normal delay epidemic models, the mathematical foundation for its deep dynamical analysis is lacked. However, the numerical simulations show that, with appropriate parameters, the system eventually approaches to the steady state on the equilibria line with different and relatively small rewiring delay, and the stable limit cycle may appear with the increase of rewiring delay. These results may provide new insights into the study of delayed network epidemic model.

## Acknowledgments

The research was partially supported by the National Natural Science Foundation of China under Grants (11331009, 61873154, 11701528), Hundred Talents Plan in Shanxi Province, the NSERC of Canada, Universities' Science and Technology Innovation Item of Shanxi Province 2019L0472, Graduate Students' Education Innovation Item of Shanxi Province 2016BY120.

The authors would like to thank the reviewers for their valuable suggestions.

## Conflict of interest

All authors declare no conflicts of interest regarding the publication of this paper.

## References

1. M. Faloutsos, P. Faloutsos and C. Faloutsos, On power-law relationships of the internet topology, *Comput. Commun. Rev.*, **29** (1999), 251–262.

2. V. Colizza, A. Barrat, M. Barthélemy, et al., The role of the airline transportation network in the prediction and predictability of global epidemics, *Proc. Natl. Acad. Sci. USA*, **103** (2006), 2015–2020.
3. M. E. J. Newman, The structure of scientific collaboration networks, *Proc. Natl. Acad. Sci. USA*, **98** (2001), 404–409.
4. M. E. J. Newman, Scientific collaboration networks. I. Network construction and fundamental results, *Phys. Rev. E*, **64** (2001), 016131.
5. P. L. Krapivsky, S. Redner and F. Leyvraz, Connectivity of growing random networks, *Phys. Rev. Lett.*, **85** (2000), 4629–4632.
6. S. N. Dorogovtsev and J. F. F. Mendes, Scaling properties of scale-free evolving networks: Continuous approach, *Phys. Rev. E*, **63** (2001), 056125.
7. G. Kossinets and D. J. Watts, Empirical analysis of an evolving social network, *Science*, **311** (2006), 88–90.
8. A. Clauset, C. R. Shalizi and M. E. J. Newman, Power-law distributions in empirical data, *SIAM Rev.*, **51** (2009), 661–703.
9. M. Kivela, A. Arenäs, M. Barthélemy, et al., Multilayer network, *J. Comp. Net.*, **2** (2014), 203–271.
10. S. Boccaletti, G. Bianconi, R. Criado, et al., The structure and dynamics of multilayer networks, *Phys. Rep.*, **544** (2014), 1–122.
11. V. Colizza and A. Vespignani, Invasion threshold in heterogeneous metapopulation networks, *Phys. Rev. Lett.*, **99** (2007), 148701.
12. N. Masuda, Effects of diffusion rates on epidemic spreads in metapopulation networks, *New J. Phys.*, **12** (2010), 093009.
13. W. K. V. Chan and C. Hsu, Service scaling on hyper-networks, *Serv. Science*, **1** (2009), 17–31.
14. A. Trilla, G. Trilla and C. Daer, The 1918 "Spanish flu" in Spain, *Clin. Infect. Dis.*, **47** (2008), 668–673.
15. M. A. Marra, S. J. Jones, C. R. Astell, et al., The genome sequence of the SARS-associated coronavirus, *Science*, **300** (2003), 1399–1404.
16. J. S. Peiris, S. T. Lai, L. L. Poon, et al., Coronavirus as a possible cause of severe acute respiratory syndrome, *Lancet*, **361** (2003), 1319–1325.
17. T. R. Frieden, I. Damon, B. P. Bell, et al., Ebola 2014—new challenges, new global response and responsibility, *New Engl. J. Med.*, **371** (2014), 1177–1180.
18. W. O. Kermack and A. G. McKendrick, Contributions to the mathematical theory of epidemics, *Proc. Roy. Soc. A*, **115** (1927), 700–721.
19. N. T. J. Bailey, The mathematical theory of infectious diseases and its applications, Hafner Press, New York, 1975.
20. R. Anderson and R. May, Infectious disease of human: dynamic and control, Press Oxford, Oxford University, 1991.

21. M. Martcheva, *Introduction to Mathematical Epidemiology*, Springer-Verlag, New York, 2010.
22. I. Al-Darabsah and Y. Yuan, A time-delayed epidemic model for Ebola disease transmission, *Appl. Math. Comput.*, **290** (2016), 307–325.
23. A. S. Klovdahl, Social networks and the spread of infectious diseases—the AIDS example, *Soc. Sci. Med.*, **21** (1985), 1203–1216.
24. R. M. May and R. M. Anderson, Transmission dynamics of HIV infection, *Nature*, **326** (1987), 137–142.
25. O. Diekmann, M. C. M. De Jong and J. A. J. Metz, A deterministic epidemic model taking account of repeated contacts between the same Individuals, *J. Appl. Prob.*, **35** (1998), 448–462.
26. Y. Moreno, R. Pastor-Satorras and A. Vespignani, Epidemic outbreaks in complex heterogeneous networks, *Euro. Phys. J. B*, **26** (2002), 521–529.
27. E. Volz, SIR dynamics in random networks with heterogeneous connectivity, *J. Math. Biol.*, **56** (2008) 293–310.
28. C. T. Bauch, The spread of infectious diseases in spatially structured populations: an invasy pair approximation, *Math. Biosci.*, **198** (2005), 217–237.
29. C. Moore and M. E. J. Newman, Epidemics and percolation in small-world networks, *Phys. Rev. E*, **61** (2000), 5678–5682.
30. R. Pastor-Satorras and A. Vespignani, Epidemic dynamics and endemic states in complex networks, *Phys. Rev. E*, **63** (2001) 066117.
31. N. M. Ferguson, D. A. T. Cummings, C. Fraser, et al., Strategies for mitigating an influenza pandemic, *Nature*, **442** (2006), 448–452.
32. T. Gross, C. J. D. Linares and B. Blasius, Epidemic Dynamics on an Adaptive Network, *Phys. Rev. Lett.* **96** (2006), 208701.
33. D. H. Zanette and S. Risau-Gusmán, Infection spreading in a population with evolving contacts, *J. Biol. Phys.*, **34** (2008), 135–148.
34. L. B. Shaw and I. B. Schwartz, Fluctuating epidemics on adaptive networks, *Phys. Rev. E* **77** (2008), 066101.
35. A. Szabó-Solticzky, L. Berthouze, I. Z. Kiss, et al., Oscillating epidemics in a dynamic network model: stochastic and mean-field analysis, *J. Math. Biol.* **72** (2016), 1153–1176.
36. J. Li, Z. Jin, Y. Yuan, et al., A non-Markovian SIR network model with fixed infectious period and preventive rewiring, *Comput. Math. Appl.*, **75** (2018), 3884–3902.
37. I. Z. Kiss, L. Berthouze, T. J. Taylor, et al., Modelling approaches for simple dynamic networks and applications to disease transmission models, *Proc. R. Soc. A*, **468** (2012), 1332–1355.
38. T. Rogers, W. Clifford-Brown, C. Mills, et al., Stochastic oscillations of adaptive networks: application to epidemic modelling, *J. Stat. Mech.*, **2012** (2012), P08018.
39. S. Risau-Gusman and D. H. Zanette, Contact switching as a control strategy for epidemic outbreaks, *J. Theor. Biol.*, **257** (2009), 52–60.
40. M. J. Keeling, The effects of local spatial structure on epidemiological invasions, *Proc. R. Soc. Lond. B*, **266** (1999), 859–867.



41. X. Zhang, C. Shan, Z. Jin, et al., Complex dynamics of epidemic models on adaptive networks, *Journal of differential equations, J. Differ. Equations*, **266** (2019), 803–832.
42. J. Graef, M. Li and L. Wang, A study on the effects of disease caused death in a simple epidemic model, in *Dyn. Syst. Differ. Equations* (eds. W. Chen and S Hu), Southwest Missouri State University Press, (1998), 288–300.
43. M. Y. Li, W. Liu, C. Shan, et al., Turning Points And Relaxation Oscillation Cycles in Simple Epidemic Models, *SIAM J. Appl. Math.*, **76** (2016), 663–687.



AIMS Press

©2019 the Author(s), licensee AIMS Press. This is an open access article distributed under the terms of the Creative Commons Attribution License (<http://creativecommons.org/licenses/by/4.0>)